Characterization of the Solidification Path and Microstructure of AlSi7Cu3Mg0.3 Alloy with Gd Content

O. Gursoy, G. Scampone

Al-Si-Cu alloys are widely used in the power train production, such as engine block and cylinder head. Since the service temperature of those parts is higher than 200°C, a thermally stable microstructure is essential. Gd has a potential to form secondary phases which may retard the coarsening behaviour in microstructure. In this study, the effect of Gd addition on the solidification path and microstructural evolution of AlSi7Cu3Mg0.3 alloy was investigated. Thermal analyses and microstructural investigation techniques were performed to evaluate the changes associated with Gd content. The results show that although Gd is ineffective on grain refinement, it can refine the eutectic Si crystals. The addition of Gd leads to the formation of $GdAl_2Si_2$ and $Gd_3Al_2Si_3Cu_2$ phases, which may improve the thermal stability of the alloy at high temperatures.

KEYWORDS: AL-SI ALLOY, SOLIDIFICATION, GADOLINIUM, HIGH TEMPERATURE, THERMAL STABILITY

INTRODUCTION

Since light weighting is one of the most effective method to decrease the fuel consumption and CO_2 emission, the importance of aluminium alloys in automotive and aerospace industry is gradually increasing. Al-Si alloys are widely used in automotive industry, especially for the power train production, such as engine block, cylinder head, etc. Advanced mechanical properties are directly related to the microstructure of the alloys, and they can be enhanced by preliminary molten metal treatments and the addition of some alloying elements. The mechanical performances of Al-Si alloys can be significantly improved by alloying with Cu and Mg. However, Cu- and Mg-rich phases can only be effective at temperatures below 200°C, due to the dissolution and coarsening phenomena that occur at higher temperatures and reduce the mechanical performance of the alloy [1].

To improve the high-temperature mechanical properties of Al–Si alloys, it is necessary to induce the formation of thermally stable and coarsening resistant precipitates in the microstructure.

Rakhmonov et al. [2] reviewed the effect of adding transition elements on the high-temperature behavior

Ozen Gursoy,
Giulia Scampone
University of Padova,
Department of Management and Engineering
yozen.gyursoy@phd.unipd.it;
giulia.scampone@phd.unipd.it

of Al-Si alloys. These elements, such as Zr, V, Ti, lead to the formation of fine and homogenously distributed precipitates, which are more coarsening resistant and thermally stable than the traditional secondary Mg_2Si and Al_2Cu precipitates. The addition of rare earth (RE) has also a beneficial impact on the high-temperature tensile properties of Al-Si alloys. Stroh et al. [3] reported that the precipitation of AlSiRE and $Al_{20}Ti_2RE$ intermetallics in RE-modified A356 alloy allows a significant increase of the yield and tensile strength at 250 °C and 300 °C.

Among rare earth elements, Gadolinium (Gd) has low diffusivity and solid solubility in α-Al [4], and it can positively influence the mechanical performance of Al alloys at high service temperatures by forming thermally stable secondary phases. Previous studies show that the addition of Gd refines α-Al grains and modifies eutectic Si crystals [5,6]. Despite those studies, the effect of Gd addition on Al-Si alloys for high temperature performance has not been investigated in detail. To compensate this lack of knowledge, the present work aims to characterize the effect of Gd content on the solidification path and the microstructure of AlSi7Cu3Mg0.3 alloy.

EXPERIMENTAL PROCEDURE

Primary AlSi7Mg0.3 alloy in the form of commercial ingots was melted by using SiC crucible in an electrical resistance furnace at 750°C. The melt was then alloyed with commercially pure Cu wires to achieve the desired content of 3 wt. % in AlSi7Cu3Mg0.3 alloy. AlGd5 waffle-shaped master alloy was added, when necessary, to increase the concentration of Gd. The chemical compositions of the experimental alloys were measured by optical emission spectrometry (OES) and presented in Table 1. Some other elements, such as Ca, Cr, P, Zr, Bi, Pb, Sb and Sn, are present in an amount of less than 0.005 wt. % and these elements are not reported in Table 1. After the additions, the molten metal was held at 750°C for 45 minutes to ensure the complete dissolution of the master alloy [7]. The melt was then carefully skimmed, stirred and poured into a boron nitride-coated truncated conical steel cup (lower diameter 45 mm, upper diameter 70 mm, height 60 mm, and a uniform wall thickness of 1 mm). The cup was preheated at 550 °C. No degassing was performed in the experimental work.

Tab.1 - Chemical composition of the experimental alloys (wt. %).

Alloy	Si	Cu	Mg	Fe	Ti	Mn	Ni	Sr	Na	Gd	Al
AlSi7Cu3Mg0.3	7.23	3.14	0.30	0.064	0.133	0.0015	0.003	-*	-*	-	bal.
AlSi7Cu3Mg0.3Gd	7.32	3.13	0.31	0.066	0137	0.0015	0.009	-*	-*	0.28	bal.

*If present, Sr and Na were below the lower detection limit (<1ppm) of OES.

Computer aided two-thermocouple thermal analysis and differential scanning calorimetry (DSC) were performed to characterize the solidification path of the experimental alloys.

For the two-thermocouple thermal analyses method, K-type thermocouples (ø1 mm) were fixed at the lid of the cup, and they were located along the central axis and adjacent to the wall of the cup. They were covered with tight stainless-steel tubes and inserted into the melt at a depth of 30 mm below the surface of the lid. The temperature and time data were collected with a sampling rate of 0.1 s^{-1} and an accuracy of 0.1 °C using a high-speed data acquisition system. The thermal analyses sample was then allowed to cool in air with a cooling rate of 0.2 °C/s. To determine the characteristic temperatures of the primary α-Al phase and Al–Si eutectic reaction, the cooling curves and the corresponding derivative curves (cooling rate) were plotted for each alloy. The nucleation temperature of Regular-Al ($T_{N,\ Al}$), the minimum temperature of α-Al ($T_{min,\ Al}$), the growth temperature of α-Al ($T_{G,\ Al}$), the recalescence undercooling of α-Al ($\Delta T_{R,\ Al}$), the eutectic nucleation temperature ($T_{N,\ eu}$), the minimum eutectic temperature ($T_{min,\ eu}$), the eutectic growth temperature ($T_{G,\ eu}$), the recalescence undercooling of eutectic ($\Delta T_{R,\ eu}$) and the nucleation temperature of Cu-rich phases ($T_{N,\ Al\text{-}Cu}$) were analyzed to estimate the efficiency of grain

refinement and eutectic modification.
The DSC analysis was carried out at a scan rate of 1°C/min for cooling conditions on cylindrical-shaped discs weighing about 35 mg and extracted from the samples used for the analysis of the chemical composition.

For the macro- and microstructural investigation, the samples were sectioned longitudinally in half and the region close to the tip of the central thermocouple was analyzed. Optical microscope (OM) and Scanning electron microscopy (SEM) equipped with energy dispersive spectrometer (EDS) were used to characterize the evolution of the microstructure and the type and morphology of the phases precipitated during the solidification. A total of at least 200 secondary dendrite arms and 2000 eutectic silicon particles were measured for each sample in OM with image analyzer for the investigation of secondary dendrite arm spacing (SDAS) and eutectic structure, respectively.
To quantitatively analyze the grain size, the polished samples were etched in the concentrated Keller's reagent (7.5 ml HNO_3, 2.5 ml HF, 5 ml HCl and 35 ml H2O). The grain size of the samples was then measured by using the intercept method (ASTM standard E112-12).

RESULT AND DISCUSSION

The cooling curves and the corresponding cooling rates obtained from the thermal analysis of the experimental alloys are shown in Figure 1. Table 2 presents a summary of the characteristic temperatures that were determined by analyzing the cooling curves and the cooling rates of the experimental alloys.
The precipitation of α-Al, Al-Si eutectic and Cu-rich phases can be easily identified in the cooling curve and cooling rate of the AlSi7Cu3Mg0.3 alloy (Figure 1a). No significant change in the precipitation of α-Al is observed after the addition of Gd, while the undercooling of Al-Si eutectic reaction in the cooling curve of AlSi7Cu3Mg0.3Gd increases (Figure 1b).
The regions of the cooling rate associated with the precipitation of eutectic Si and Cu-rich phases in Gd-containing alloy show sharper and higher peaks due to the slower release of latent heat compared to the Gd-free alloy. Indeed, the addition of Gd depresses the characteristic temperatures of Al-Si eutectic reaction, and it increases the recalescence undercooling of eutectic. However, the Gd content is ineffective on the recalescence undercooling of α-Al (Table 2). No peaks associated with the precipitation of Gd-rich phases were detected in thermal analyses, most likely due to unfavorable cooling rate and low number of Gd-rich phases in AlSi7CuMg0.3Gd alloy (Figure1b).

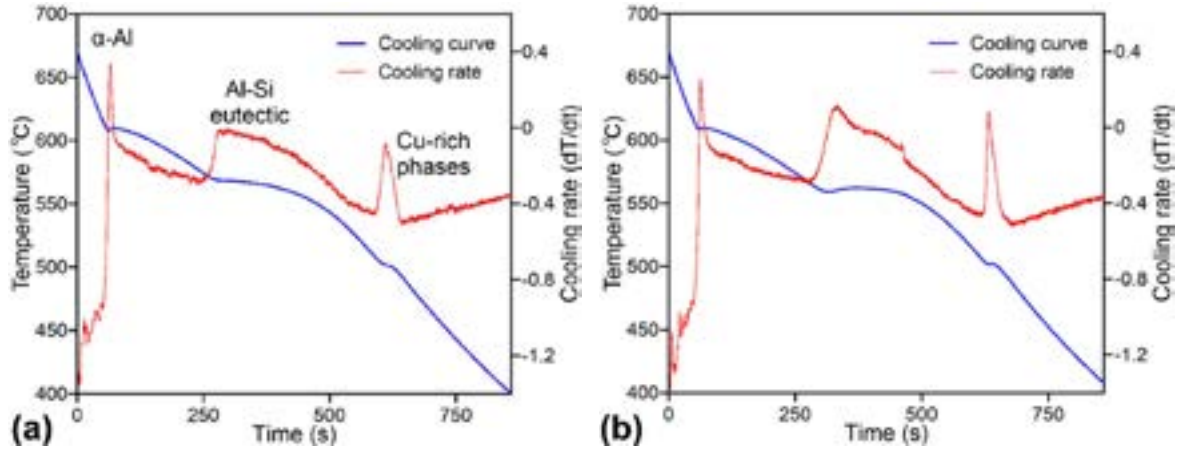

Fig.1 - Cooling curve and cooling rate of (a) AlSi7Cu3Mg0.3 and (b) AlSi7Cu3Mg0.3Gd alloys.

Tab.2 - Characteristic temperatures from thermal analysis of experimental alloys in (°C).

Alloy	$T_{N, Al}$	$T_{min, Al}$	$T_{G, Al}$	$\Delta T_{R, Al}$	$T_{N, eu}$	$T_{min, eu}$	$T_{G, eu}$	$\Delta T_{R, eu}$	$T_{N, Al-Cu}$
AlSi7Cu3Mg0.3	609.2	607.8	609.9	2.1	570.4	568.5	568.5	0	506.7
AlSi7Cu3Mg0.3Gd	610.0	608.2	609.6	1.4	562.1	559.0	562.0	3.0	503.2

DSC analyses were carried out for the experimental alloys and the cooling curves are shown in Figure 2. The cooling DSC curve of AlSi7Cu3Mg0.3 alloy exhibits the same phase reactions detected by thermal analysis, whereas DSC curve of AlSi7Cu3Mg0.3Gd alloy reveals two additional peaks (Figure 2). It is believed that those peaks are related to the precipitation of Gd-rich phases.

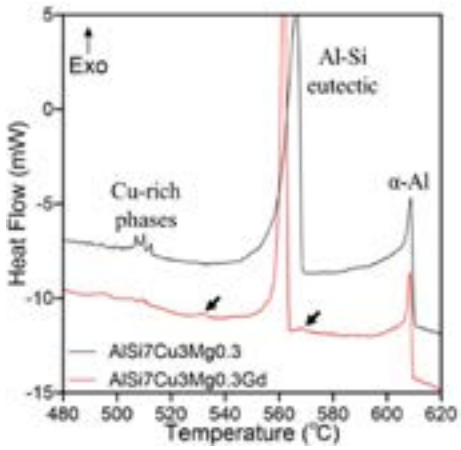

Fig.2 - Cooling DSC curves of the alloys. The arrows indicate the precipitations of the Gd-rich phases.

Figure 3 shows the macrostructures of the experimental alloys. The AlSi7Cu3Mg0.3 alloy exhibits coarse α-Al grain, most likely due to the low cooling rate of the sample (Figure 3a). After the addition of Gd, no refinement is observed in the macrostructure of AlSi7Cu3Mg0.3Gd alloy (Figure 3b).

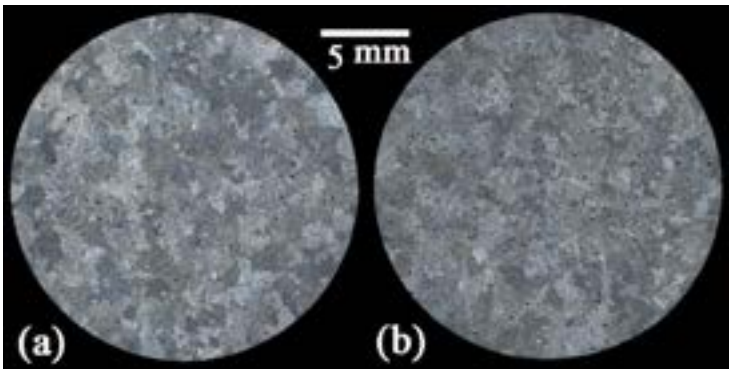

Fig.3 - Grain structure of the (a) AlSi7Cu3Mg0.3 and (b) AlSi7Cu3Mg0.3Gd alloys.

The microstructures of AlSi7Cu3Mg0.3 and AlSi7Cu3Mg0.3Gd alloys are displayed in Figure 4. Both microstructures exhibit α-Al matrix, Al-Si eutectic, θ-Al_2Cu and Q-$Al_5Si_6Cu_2Mg_8$. Additionally, Gd-rich phases appear in the AlSi7Cu3Mg0.3Gd alloy, as indicated by arrows in Figure 4b.

The AlSi7Cu3Mg0.3 alloy shows coarse, flake-like eutectic Si crystals (Figure 4a), while the eutectic structure is refined

after the addition of Gd (Figure 4b). It is well known that Sr and Na are widely used as eutectic modifiers, which lead to the formation of finer eutectic Si particles [8]. However, in the present work, these elements are not present in the chemical composition of the alloys, as reported in Table 1. Therefore, the refinement of eutectic Si can be fully attributed to the addition of Gd, which is consistent with the results reported by Shi et al. [5].

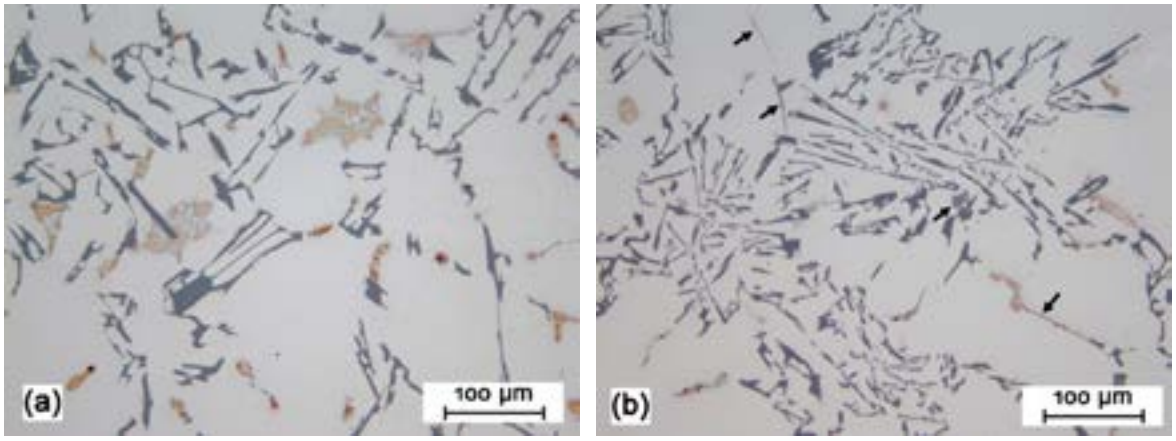

Fig.4 - Microstructure of the (a) AlSi7Cu3Mg0.3 and (b) AlSi7Cu3Mg0.3Gd alloys. The arrows indicate Gd-rich phases.

Figure 5 shows the quantitative investigations on the evolution of the macro- and microstructure of the experimental alloys. According to the quantitative analysis reported in Figure 5a, the grain size decreased from 1.3 ± 0.06 to 1.2 ± 0.08 mm after the addition of Gd. It can be noted that Gd is inefficient on grain refinement of α-Al grains. Similar results were found for secondary dendrite arm spacing (SDAS) analyses. The average SDAS value in the AlSi7Cu3Mg0.3 alloy is 74.0 ± 9.9 µm, while in the AlSi7Cu3Mg0.3Gd alloy it is 72.1 ± 10.2 µm (Figure 5a). Although Gd addition has been reported to refine α-Al phase in Al-Si alloys, no significant change in grain size or SDAS were observed after Gd addition. This can be related to the large mismatch in structure and lattice parameters between α-Al (FFC, a= 0.4049 nm) and Al_3Gd (HCP, a= 0.3634 nm, b= 0.5781 nm).

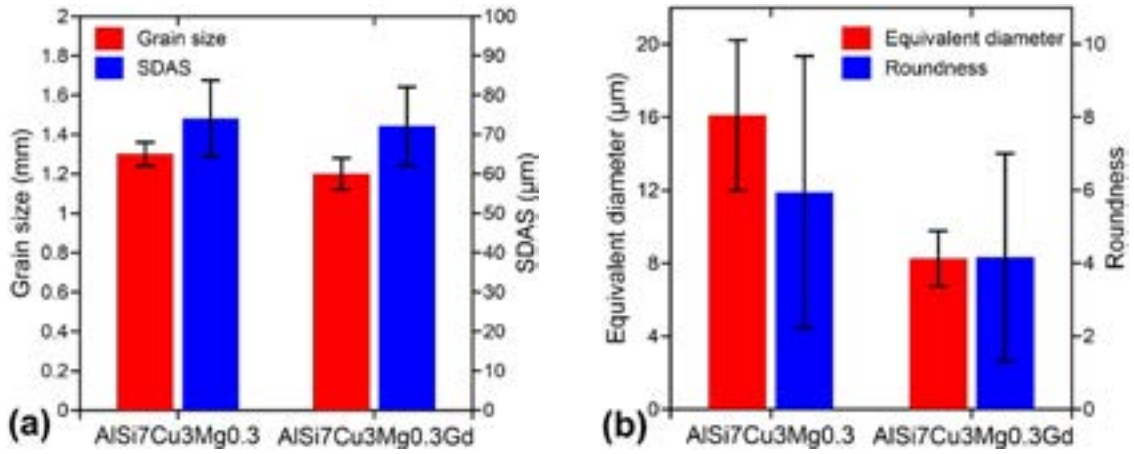

Fig.5 - Evolution of (a) the grain size, SDAS and (b) roundness and equivalent circular diameter of Si particles in the investigated alloys.

Figure 5b shows the variation of the morphological parameters of Si eutectic particles after the addition of Gd. In the AlSi7Cu3Mg0.3Gd alloy, the eutectic Si particles are refined, indeed the equivalent diameter of Si decreases from 16.1 ± 10.3 μm to 8.3 ± 3.8 μm. It is well known that AlP compounds play an important role in the precipitation of eutectic Si. They segregate at the dendrite/liquid interface and act as sites for the nucleation of eutectic Si during the growth of α-Al dendrite [8]. When Gd is added into the melt, it poisons AlP compounds by forming $GdAl_2Si_2$, and AlP can no longer react with the Si in the melt. During the solidification process, the liquid front of the eutectic cells is enriched of Gd, resulting in the refinement of the eutectic Si particles.

Figure 6 shows the SEM micrograph of the AlSi7Cu3Mg0.3Gd alloy. Eutectic Si crystals, θ-Al_2Cu and Q-$Al_5Si_6Cu_2Mg_8$ and two different Gd-rich phases were detected in the interdendritic region, and those phases were confirmed by EDS spot analyses. $GdAl_2Si_2$ were observed in a blocky shape and surrounded by $Gd_3Al_2Si_3Cu_2$, while it can also precipitate independently. Almost all Gd-rich phases tend to segregate into the interdendritic region during solidification due to the low solid solubility of Gd in α-Al matrix. It can be assumed that the pre-eutectic peak detected in the DSC curve of the Gd-containing alloy (Figure 2) is related to the precipitation of $GdAl_2Si_2$ while the post-eutectic peak corresponds to the precipitation of $Gd_3Al_2Si_3Cu_2$ phase. However, there is lack of information on $Gd_3Al_2Si_3Cu_2$ phase in the database of many solidification calculation software. Therefore, further investigation must be carried out to characterize in the detail the formation of Gd-rich compounds and to understand if these phases may have a beneficial effect on the thermal stability of the alloy at high service temperatures.

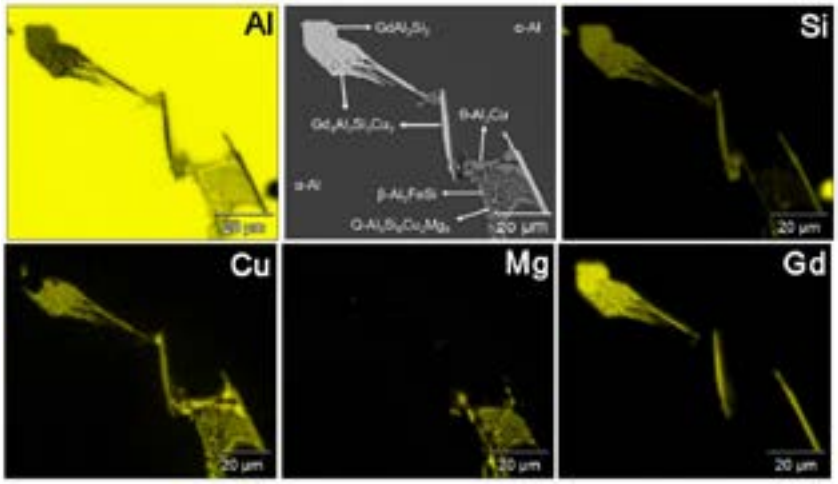

Fig.6 - Backscattered electron FEG-SEM image of Gd-rich phases in AlSi7Cu3Mg0.3Gd alloy and corresponding EDS composition maps, showing the distribution of Al, Si, Cu, Mg and Gd.

CONCLUSIONS

In this work, the effect of Gd content on the solidification path and the microstructure of AlSi7Cu3Mg0.3 alloy was investigated. The following conclusions can be drawn:

- The addition of Gd results in a refinement of eutectic Si particles while it has no effect on the size of α-Al grains.
- During the solidification of AlSi7Cu3Mg0.3 alloy, two different Gd-rich phases precipitate at pre- and post-eutectic temperatures. These phases are: $GdAl_2Si_2$ and $Gd_3Al_2Si_3Cu_2$.
- Gd-rich phases may have beneficial effect on high temperature mechanical properties, therefore further investigations should be carried out on this topic.

ACKNOWLEDGMENTS

The work was developed with the financial support of Fondazione Cassa di Risparmio di Padova e Rovigo (CariPaRo), Padova (2019).
The authors would like to thank Prof. Giulio Timelli for his invaluable feedback and support.

REFERENCES

[1] Javidani M, Larouche D. Application of cast Al–Si alloys in internal combustion engine components. Int Mater Rev. 2014; 59:132-158.
[2] Rakhmonov J, Timelli G, Bonollo F. The Effect of Transition Elements on High-Temperature Mechanical Properties of Al–Si Foundry Alloys–A Review. Adv Eng Mat. 2016, 18:1096-1105.
[3] Stroh J, Sediako D, Weiss D. The Effect of Rare Earth Mischmetal on the High Temperature Tensile Properties of an A356 Aluminum Alloy. Light Metals 2021. The Minerals, Metals & Materials Series, Springer, Cham. 2021, 184–191.
[4] Mondolfo L F, Aluminum alloys: structure and properties, Elsevier. 1979.
[5] Shi Z, Wang Q, Shi Y, Zhao G, Zhang R. Microstructure and mechanical properties of Gd-modified A356 aluminum alloys. J Rare Earths. 2015, 33:1004-1009.
[6] Liu W, Xiao W, Xu C, Liu M, Ma C. Synergistic effects of Gd and Zr on grain refinement and eutectic Si modification of Al-Si cast alloy. Mater Sci Eng A. 2017, 693:93-100.
[7] Gursoy O, Timelli, G. The effect of the holding time on the microstructure of Gd-containing AlSi7Mg alloys. In Light Metals 2022. The Minerals, Metals & Materials Series, Springer, Cham. 2022, 779-784.
[8] Gursoy O, Timelli,G. Lanthanides: a focused review of eutectic modification in hypoeutectic Al–Si alloys. J Mater Res Technol. 2020, 9:8652-8666.